Tourmaline as a petrogenetic indicator mineral: an example from the staurolite-grade metapelites of NW Maine

DARRELL J. HENRY[1]

Lunar and Planetary Institute
3303 NASA Road 1, Houston, Texas 77058

AND CHARLES V. GUIDOTTI

Department of Geological Sciences
University of Maine, Orono, Maine 04473

Abstract

Tourmaline, a mineral often overlooked in petrologic studies, is shown to be a useful petrogenetic indicator mineral. Despite the large number of possible substitutions in tourmaline, generalizations relating tourmaline composition and rock type are made. Based on available literature data, distinct regions are defined within Al–Fe(tot)–Mg and Ca–Fe(tot)–Mg diagrams for tourmaline from different rock types.

As an example of the utility of tourmaline in petrologic studies, the accessory tourmaline from staurolite-grade pelitic schists from NW Maine is investigated. These tourmaline grains typically display three general styles of chemical zoning: (1) a lack of zoning, (2) a continuous core-to-rim zonation attributed to growth during progressive metamorphism, and (3) a zonation marked by a distinct discontinuity apparently representing detrital tourmaline grains surrounded by metamorphic tourmaline overgrowths. All of the samples in this study contain Si-, Al-, and Ti-saturating phases (quartz, staurolite, and ilmenite, respectively). Consequently, the substitutional complexities of tourmaline in equilibrium with the matrix are minimized. Systematic element partitioning suggests that chemical equilibrium has been attained among the rims of the tourmaline grains and matrix minerals. Tourmaline rims have the highest Mg/Fe and Na/Ca ratios of any of the phases in the metapelites. The compositions of tourmaline cores that are presumed to be detrital in origin are optically and chemically distinct from their tourmaline overgrowths. In the Al–Fe(tot)–Mg and Ca–Fe(tot)–Mg diagrams, the compositions of the detrital cores fall in the fields of rock types that are commonly found in the presumed source region for the pelitic sediments.

Introduction

Tourmaline is a very common accessory mineral found in many rock types and terrains. It occurs in many clastic sedimentary rocks as a chemically- and mechanically-resistant heavy mineral (Krynine, 1946; Pettijohn et al., 1973), but also develops authigenically during the late stages of diagenesis (Awasthi, 1961; Ricketts, 1978; Gautier, 1979; Mader, 1980). Tourmaline is found in metamorphic rocks with a wide range of bulk compositions and develops at virtually all grades of metamorphism. In addition, granitoid intrusive rocks and their associated aplites, pegmatites, and hydrothermal aureoles commonly contain significant amounts of tourmaline. Neverthe-

less, studies on the relationship between the compositional variations of tourmaline and its petrologic significance are relatively scarce. As such, tourmaline has apparently become a "forgotten" mineral in terms of its use as a petrogenetic indicator.

This paper describes some of the crystallographic and chemical aspects of tourmaline which provide a basis for systematic petrologic studies of tourmaline. Additionally, some generalizations are made concerning the relationships between tourmaline composition and rock type (based on data from the literature). Furthermore, to illustrate the usefulness of tourmaline studies, the compositional variations of tourmaline in staurolite-grade pelitic schists from northwestern Maine are investigated. These tourmalines are examined to determine such factors as their chemical zonation patterns, their approach to chemical equilibrium, and their relative element partitioning

---

[1] Present address: Arco Oil and Gas Company, 2300 Plano Parkway, Plano, Texas 75023.

with coexisting phases. These data are used to make inferences concerning the origin of tourmaline in these metasediments and the development of the chemical zoning patterns in the tourmaline.

General aspects of tourmaline mineral chemistry

Tourmaline is a complex borosilicate mineral with a general formula of $XY_3Z_6(BO_3)_3Si_6O_{18}(OH)_4$. It has two types of octahedral sites: the Z site and a slightly larger, more distorted Y site (Donnay and Barton, 1972; Rosenberg and Foit, 1979). The Z site is typically occupied by Al but significant amounts of Fe^{2+}, Fe^{3+}, Ti, Mg, Cr, and V^{3+} can replace Al (Barton, 1969; Tsang et al., 1971; Gorelkova et al., 1978; Foit and Rosenberg, 1979; Korovushkin et al., 1979; Nuber and Schmetzer, 1979; Burns, 1982). The larger Y site tolerates extensive and diverse substitutions involving monovalent, divalent, trivalent, and quadrivalent cations (Frondel et al., 1966; Hermon et al., 1973; Fortier and Donnay, 1975; Foit and Rosenberg, 1979). The X site usually contains Na but may also accommodate variable amounts of Ca, Mg, and vacancies (Foit and Rosenberg, 1977). Boron is in regular triangular coordination and has no apparent substituents (Tsang and Ghose, 1973; Povondra, 1981). Some Al can substitute for Si in the tetrahedral site (Foit and Rosenberg, 1979). Finally, in the hydroxyl site F^- or O^{2-} can substitute for OH^- (Nemec, 1968; Foit and Rosenberg, 1977).

Because of the large amount of potential substitution, tourmaline is usually considered in terms of its common end-member components (Table 1). To a great extent, most natural tourmalines belong to two completely miscible solid solution series: schorl-dravite and schorl-elbaite. However, an apparent miscibility gap exists between

Table 1. Common tourmaline end members

End member	Formula
Schorl	$NaFe^{2+}_3Al_6(BO_3)_3Si_6O_{18}(OH)_4$
Dravite	$NaMg_3Al_6(BO_3)_3Si_6O_{18}(OH)_4$
Tsiliasite	$NaMn_3Al_6(BO_3)_3Si_6O_{18}(OH)_4$
Elbaite	$Na(Li,Al)_3Al_6(BO_3)_3Si_6O_{18}(OH)_4$
Uvite	$CaMg_3(MgAl_5)(BO_3)_3Si_6O_{18}(OH)_4$
Liddicoatite	$Ca(Li,Al)_3Al_6(BO_3)_3Si_6O_{18}(OH)_4$
Alkali-defect tourmaline	$\Box(Y^{2+}_2,Y^{3+})Al_6(BO_3)_3Si_6O_{18}(OH)_4$ [*]
Proton-deficient tourmaline	$NaY^{3+}_3Al_6(BO_3)_3Si_6O_{22}(OH)$
Buergerite	$NaFe^{3+}_3Al_6(BO_3)_3Si_6O_{22}F$
Ferridravite	$NaMg_3Fe^{3+}_6(BO_3)_3Si_6O_{18}(OH)_4$

[*] Y^{2+} and Y^{3+} represent any divalent or trivalent cation, respectively, in the Y site. Consequently, the actual end member will depend on the cation chosen for the Y site.

Table 2. Important substitutional schemes and exchange components in tourmaline

Site substitutions	Exchange components
(1) Fe^{2+}_Y [*] $= Mg_Y$	$MgFe_{-1}$
(2) $Na_X + Al_Z = Ca_X + Mg_Z$ uvite substitution	$CaMgNa_{-1}Al_{-1}$
(3) $Na_X + Al_Y = Ca_X + Fe^{2+}_Y$	$CaMgNa_{-1}Al_{-1}$
(4) $Na_X + Al_Y = Mg_X + Fe^{2+}_Y$	$Mg_2Na_{-1}Al_{-1}$
(5) $Na_X + Al_Y = Ca_X + Li_Y$ liddicoatite substitution	$CaLiNa_{-1}Al_{-1}$
(6) $Mg_Y + Si_T = Al_Y + Al_T$ tschermaks substitution	$Al_2Mg_{-1}Si_{-1}$
(7) $Na_X + Mg_Y = Al_Y + \Box_X$ [**] alkali-defect substitution	$AlNa_{-1}Mg_{-1}$
(8) $Mg_Y + OH^- = Al_Y + O^2$ aluminobuergerite substitution	$AlMg_{-1}H_{-1}$
(9) $Fe^{2+}_Y + OH^- = Fe^{3+}_Y + O^{2-}$ buergerite substitution	H_{-1}
(10) $Al_Z = (Fe^{3+},Cr^{3+},V^{3+})_Z$	$FeAl_{-1}, CrAl_{-1}, VAl_{-1}$
(11) $Mg_Y + 2Si_T = Ti_Y + 2Al_T$	$TiAl_2Mg_{-1}Si_{-2}$
(12) $2Fe^{2+}_Y = Li_Y + Al_Y$ elbaite substitution	$LiAlFe_{-2}$
(13) $OH^- = F^-$	FOH_{-1}

[*] The subscripts represent the alkali site(X), the two octahedral sites (Y and Z), and the tetrahedral site(T) in the general structural formula.

[**] This symbol represents a vacancy in the X site.

dravite and elbaite (Deer et al., 1962). For this reason, tourmalines are typically described in terms of their position in the elbaite-schorl series or in the schorl-dravite series. Nonetheless, there can be considerable deviation from compositions describable by these end member components alone. In some tourmalines there are significant amounts of the uvite component (cf. Dunn et al., 1977b). Most natural tourmalines also contain significant amounts of the alkali-free and proton-deficient tourmaline components (Foit and Rosenberg, 1977; Rosenberg and Foit, 1979). In addition, the tsiliasite component can be important in tourmalines which are predominantly in the elbaite-schorl solid solution series (Slivko, 1959). Finally, those tourmalines containing significant amounts of Fe^{3+} will have appreciable buergerite and/or ferridravite components (Frondel et al., 1966; Jones et al. 1981).

Substitutions in tourmaline can take place as homovalent cation exchanges on a single site (such as Mg for Fe^{2+} in the Y site) or as heterovalent coupled substitutions over several sites (such as the coupled uvite substitution (Ca–Mg for Na–Al) involving the X and Z sites). Some of the most important substitutional schemes that can give rise to the commonly observed tourmaline compositions are compiled in Table 2. Alternatively, each

of these substitutions can be expressed in terms of their corresponding exchange components (cf. Thompson, 1982). Such a formalism is useful because all of the compositional variations in tourmaline can be taken into account by selecting an end-member (additive) component and introducing the appropriate exchange components (Thompson et al., 1982).

The complex chemical variability of tourmaline and its relation to coexisting phases can potentially make tourmaline an indicator of the local environment in which it formed. With careful consideration of the rock system, changes in tourmaline composition can be related to such factors as the bulk composition of the host rock, the composition of coexisting minerals, and the $P-T-fo_2$ conditions. In fact, because tourmaline is so mechanically and chemically stable, each tourmaline grain can potentially provide important information on the history of the rock in which it is found.

Tourmaline composition versus rock type

Despite the large number of permissable substitutions, some generalizations can be made about the relationship between tourmaline composition and the host rock type. As is apparent from Table 2, four of the most important substituent elements are Al, Ca, Fe, and Mg. A review of available literature (see Appendix 1) shows that if tourmaline compositions from various rock types are plotted on Al–Fe(tot)–Mg and Ca–Fe(tot)–Mg ternary diagrams, several distinct regions can be defined for tourmalines from different rock types (Figs. 1 and 2). Some imprecision in locating boundaries between rock types results from tourmaline analyses which were performed on mineral separates representing the bulk composition of tourmalines (often zoned or containing undetected mineral inclusions (cf. Dunn, 1977)). In addition, in zoned tourmalines with complex histories, the composition of the tourmaline in equilibrium with the coexisting minerals may be only a small volume of the total tourmaline grain. Consequently, care must be taken in evaluating the tourmaline composition in equilibrium with the matrix minerals.

These types of diagrams are useful for the following reasons: (1) The plotting parameters are easily obtainable from microprobe analyses. (2) There is no reliance on a
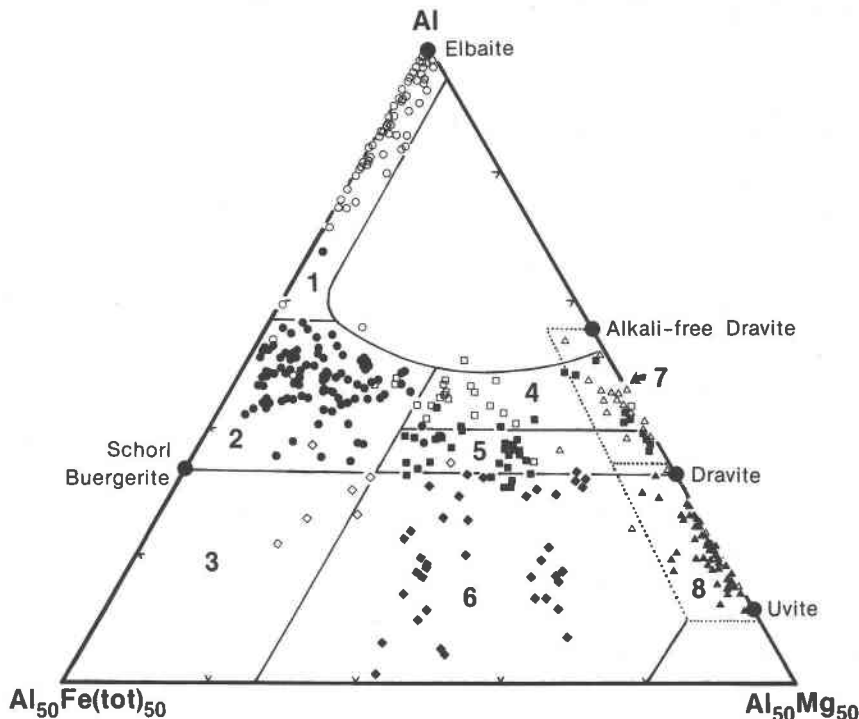

Fig. 1. Al–Fe(tot)–Mg diagram (in molecular proportions) for tourmalines from various rock types. Fe(tot) represents the total Fe in the tourmaline. Several end members are plotted for reference. This diagram is divided into regions that define the compositional range of tourmalines from different rock types. The rock types represented are (the values in brackets being the number of data points used to define the field): (1) Li-rich granitoid pegmatites and aplites [106] (○), (2) Li-poor granitoids and their associated pegmatites and aplites [98] (●), (3) Fe^{3+}-rich quartz-tourmaline rocks (hydrothermally altered granites) [7] (◇), (4) Metapelites and metapsammites coexisting with an Al-saturating phase [21] (□), (5) Metapelites and metapsammites not coexisting with an Al-saturating phase [45] (■), (6) Fe^{3+}-rich quartz-tourmaline rocks, calc-silicate rocks, and metapelites [38] (◆), (7) Low-Ca metaultramafics and Cr,V-rich metasediments [23] (△), and (8) Metacarbonates and meta-pyroxenites [55] (▲). Note the overlap of fields 4 and 5 with field 7.
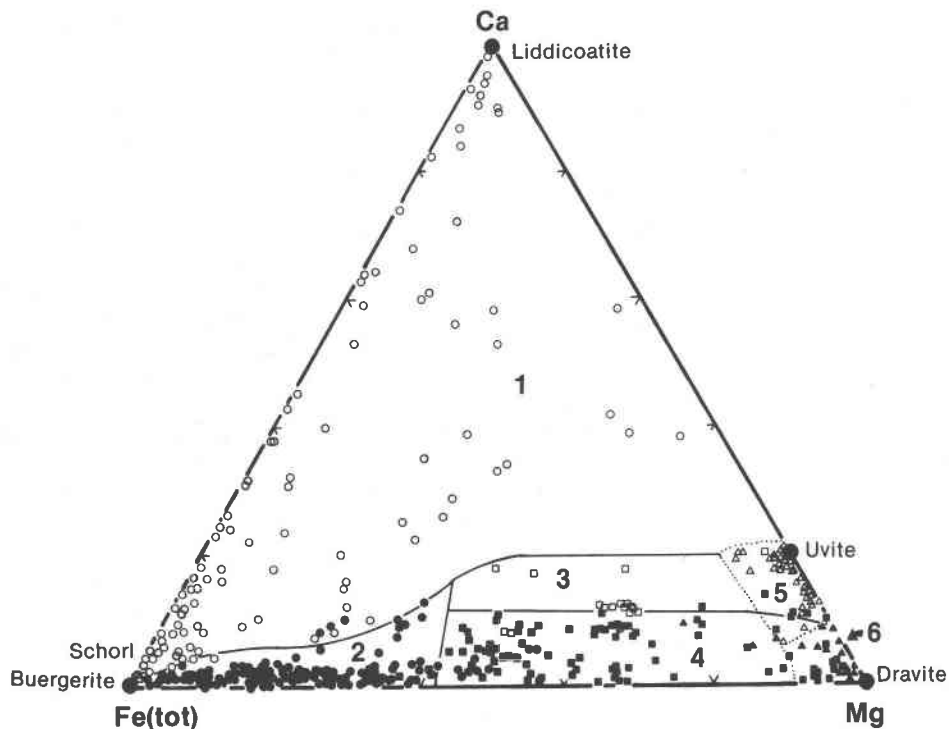
Fig. 2. Ca–Fe(tot)–Mg diagram (molecular proportions) for tourmaline from various rock types. Several of the common end members are plotted for reference. The rock types defined by the fields in this diagram are somewhat different than those in Figure 1. These fields are (the number of data points are given in the brackets): (1) Li-rich granitoid pegmatites and aplites [128] (O), (2) Li-poor granitoids and associated pegmatites and aplites [146] (●), (3) Ca-rich metapelites, metapsammites, and calc-silicate rocks [36] (□), (4) Ca-poor metapelites, metapsammites, and quartz-tourmaline rocks [69] (■), (5) Metacarbonates [54] (△), and (6) Metaultramafics [14] (▲). Note the overlap of field 4 with field 6.

particular structural formula normalization scheme. (3) The variations of the data on this diagram represent the cumulative effect of several substitutions. (4) These cations cover compositions and substitutions that are likely to be found in the the tourmalines of common rock types. (5) Some inferences can be made about cations which cannot be directly measured on the microprobe. For instance, due to its charge coupling with Al in the Y site, Li can be assumed to be present in significant amounts in the Al-rich tourmalines in region 1 of Figure 1. In addition, the presence of substantial amounts of Fe^{3+} can be inferred if the tourmaline composition falls below the schorl-dravite line i.e. Fe^{3+} is a likely major substituent of Al in the Z site assuming there is also not a substantial uvite component (Frondel et al., 1966; Barton, 1969; Hermon et al., 1973; Dunn et al., 1977b; Walenta and Dunn, 1979).

There are also disadvantages to these types of diagrams. (1) They do not directly take into account cations such as V, Cr, or Mn which can be found in significant quantities in some tourmalines. Nonetheless, the presence of some of these cations in tourmaline can be used as an additional discriminating factor for certain rock types. (2) Those tourmalines developed due to hydrothermal alteration of a pre-existing rock or pegmatite vein injec-

tion can often be difficult to systematize according to this scheme because they partially-to-completely take on the chemical characteristics of the host rock. In some cases this may produce apparently anomalous tourmaline compositions according to the defined regions. However, even these tourmalines can potentially give some information about the nature of the protolith (Benjamin, 1969; Fieremans and Paepe, 1982). For example, hydrothermal tourmaline in a rock which was originally a rhyolite will be more enriched in iron than hydrothermal tourmaline from a rock which was originally a metasediment (Black, 1971; Holgate, 1977).

If the defined fields are valid, then knowledge of the composition of a tourmaline from an unknown source should permit a reasonable evaluation of the original rock type in which it formed. Clearly, many more detailed microprobe analyses from different rock types are required to refine these diagrams.

Tourmaline from staurolite-grade schists, NW Maine

Geologic setting

Tourmaline is present in trace amounts in most of the metasediments from the Silurian Rangeley and Perry

Mountain Formations and the Ordivician Greenvale Cove and Quimby Formations of the Rangeley quadrangle of northwestern Maine (see Fig. 1 of Guidotti, 1974). In general, these formations are composed of interbedded metapelite, feldspathic metasandstone, polymictic meta-conglomerate, and calc-silicate (Moench and Zartman, 1976). They are part of a series of units in the Merrimack synclinorium, a major northeast-trending tectonic feature that reflects the Lower Devonian Acadian orogen in the northern Appalachians (Osberg, 1978).

The metamorphic history of the study area is complex with at least three episodes of Devonian regional metamorphism, two distinct deformations, and subsequent relatively minor deformational events (Moench and Zartman, 1976; Holdaway et al., 1982). Textural and chemical evidence, however, suggests that overall equilibrium was attained in the pelitic schists during the final regional metamorphic event (Guidotti, 1970, 1974; Henry, 1981).

The tourmalines discussed below are in graphite-bearing pelitic schists collected from a small area (most samples from a one km² area) within the staurolite zone. Consideration of this spatially-restricted series of samples permits evaluation of the element partitioning systematics under nearly isothermal ($T = 525 \pm 15°C$) and isobaric ($P = 3.5 \pm 0.2$ kbar) conditions (Henry, 1981).

Petrography

Tourmaline is found as a euhedral, rod-shaped, accessory mineral (trace to 2%) that is usually disseminated throughout the metapelites. Higher concentrations of tourmaline are often found in very mica-rich layers. Grains up to 400 μm in diameter have been noted but the typical size of a tourmaline grain (perpendicular to the c-axis) is approximately 50 μm. Tourmaline has been observed as an inclusion phase in most of the other minerals and, as such, apparently represents a relict detrital and/or early-formed metamorphic mineral.

Tourmaline grains are typically zoned with black to blue-green cores, frequently with numerous quartz inclusions. The rims are yellow-brown in pyrrhotite-rich rocks or green-blue in pyrrhotite-poor rocks. The color change from the core to rim may be gradational or involve sharp optical discontinuities (Fig. 3). Some tourmaline grains showing these optical discontinuities have irregular cores overgrown by euhedral rims whereas others have both euhedral cores and rims. Similar textural relations have been previously ascribed to the secondary growth of metamorphic tourmaline on detrital tourmaline fragments (Wadhawan and Roonwal, 1977; Zen, 1981). Optically unzoned tourmaline grains frequently coexist with strongly-zoned tourmaline grains in the same sample. In some cases this may be the consequence of the cut through different tourmaline grains. These textural relations suggest that there must have been some overgrowth on pre-existing tourmaline as well as nucleation and growth of new tourmaline during the metamorphism.
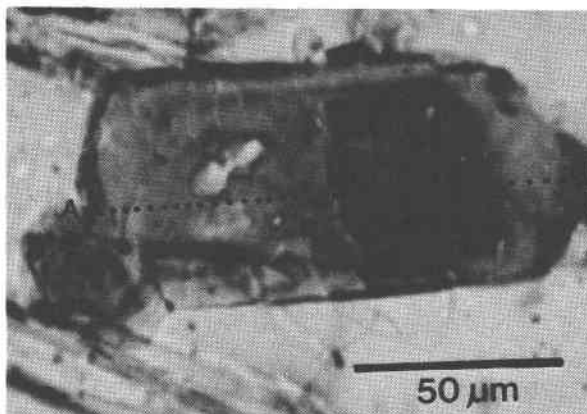

Fig. 3. Example of a tourmaline with discontinuous optical zoning. A microprobe traverse was done along section A–A' (see Fig. 4).

All of the samples considered in this study contain Al-, Si-, and Ti-saturating phases (staurolite, quartz, and ilmenite, respectively) (cf. Thompson, 1972; Thompson et al., 1977). Because these phases contain essentially fixed contents of Al, Si, and Ti, respectively, the coexisting phases are buffered to high (though not necessarily maximum), nearly constant levels of these elements under fixed pressure and temperature conditions. Three different assemblages are utilized (all containing quartz + muscovite + plagioclase (An_3–An_{22}) + ilmenite + tourmaline + apatite + graphite + pyrrhotite): (1) staurolite + biotite + garnet + chlorite, (2) staurolite + biotite + chlorite, and (3) staurolite + biotite + cordierite. The presence of graphite in the pelitic schists is indicative of relatively low fo_2 conditions. Calculations of metamorphic fluid compositions indicate that the fo_2 is slightly higher than the QFM buffer and has relatively little variation in different samples (Henry, 1981; Henry and Guidotti, 1981). These samples do, however, contain variable amounts of pyrrhotite and the sulfide-silicate interactions have a marked effect in producing a range of Mg/Fe ratios in tourmaline as well as in other ferromagnesian minerals in the samples (Henry and Guidotti, 1981, 1982).

In limiting mineral assemblages such as those given above the amount of chemical variation in tourmaline due to local differences in bulk composition is minimized. The coexistence of an Al-saturating phase (staurolite) with biotite and plagioclase necessitates that the tschermaks (6), alkali-defect (7), and aluminobuergerite (8) substitutions (see Table 2) involving Al must be held at nearly fixed levels in the tourmaline rims. In addition, because Al is buffered and there is a low and relatively small range in plagioclase compositions, there is not likely to be an appreciable amount of uvite (2) substitution. The presence of ilmenite also buffers substitution (11) to constant

levels. The low and nearly uniform fo_2 conditions inferred from the presence of graphite and from fluid phase calculations suggest that the buergerite substitution (9) will also tend to be minor. The absence of significant amounts of Fe^{3+}, Cr^{3+}, and V^{3+} in the tourmalines implies that substitution (10) is also not important. Finally, since tourmalines in the schorl-dravite series with even small amounts of the dravite component have very little Li (Foit and Rosenberg, 1977; Wilson and Long, 1983), the liddicoatite (5) and elbaite (12) substitutions are also minimal. Under these conditions only substitution (1) and, to a lesser extent, substitutions (3), (4), and (13) are potentially variable substitutions in the tourmaline in equilibrium with the matrix phases. As a consequence, the tourmaline substitutional complexities have become considerably simplified. In terms of exchange components this reduces the number of independently variable components in tourmaline to $MgFe_{-1}$, $CaMgNa_{-1}Al_{-1}$, and $Mg_2Na_{-1}Al_{-1}$, and FOH_{-1}. The range of Mg/Fe ratios in these minerals produced by the sulfide-silicate interactions make it especially useful to investigate the variation of the $MgFe_{-1}$ component under nearly constant $P-T$ conditions.

Analytical techniques

Electron microprobe analyses of tourmaline and the coexisting minerals in the pelitic schists were performed on a three-channel ARL-EMX electron microprobe at the University of Wisconsin-Madison. Anhydrous oxides and simple silicates were used as probe standards. Analyses were performed utilizing the general techniques of Bence and Albee (1968) with the alpha corrections factors of Albee and Ray (1970). Replicate analyses of secondary mineral standards provided a measure of the magnitude of the error associated with the analytical precision (Henry, 1981). For example, the relative uncertainty in the precision of the Mg/Fe ratios of biotite is ±0.5%. These analytical uncertainties are taken into account in evaluating the chemical zoning and element partitioning data.

Analysis of tourmaline requires some additional considerations. First, the fine-grained nature and the strong chemical zoning made it necessary to obtain the analysis on as small an area as possible. As such the beam was tightly focussed to a 1–3 μm spot. Repeated analysis on a single spot showed little variation with time. Consequently, there appears to be minimal B-loss due to volatilization under the electron beam. Second, B, Li, and H cannot be directly measured on the probe. However, inasmuch as boron is the only cation to be expected in regular triangular coordination (Tsang and Ghose, 1973) it is assumed that there are 3 boron atoms in the structural formula and the weight percent of B_2O_3 necessary to produce the 3 boron atoms was calculated for each analysis. Since the amount of H_2O is still not known, the structural formula is calculated on the basis of 29 oxygens. This tacitly assumes that there is full occupancy of 4 hydroxyl anions in the hydroxyl site. Those tourmalines that contain an appreciable amount of trivalent cations in the Y site or F in the hydroxyl site will contain less than 4 hydroxyl anions. Nonetheless this approach provides a reasonable starting point with which to observe substitutional trends.

Analytical results

Chemical zoning. The tourmalines in the metapelites display three types of chemical zonation: (1) apparently homogeneous compositional patterns (relatively rare), (2) a continuous core-to-rim zoning where Al, Mg, and Ca increase as Fe, Na, Si, and typically Ti decrease (most common), and (3) a discontinuous zoning profile often marked by steep concentration gradients and no systematic core-to-rim zoning patterns (common). Representative microprobe analyses of various portions of the zoned tourmalines are presented in Table 3.

The rim-to-rim compositional profile of Figure 4 across a tourmaline grain containing an optically-discontinuous core is an example of the complex zoning patterns that often develop in type (3) tourmaline grains. From the rim toward the core there is an overall continuous compositional zoning pattern such that Fe and Si increase as Mg and Al decrease until the optically distinct core is encountered. Near the boundary of the optical discontinuity there is a strong concentration gradient in which Al decreases abruptly as Fe, Ti, Na, and Si increase. At the center of the core there is, in fact, not enough Al to fill the Z site. Because the Ca and Mg do not increase significantly, the most likely substitution is one in which Fe^{3+} substitutes for Al in the Z site. Clearly this optically distinct core formed in an environment which was different from the environment in which the outer portion of the grain equilibrated. The outer continuous zoning may represent the metamorphic zoning developed during progressive metamorphism and possibly later modified somewhat by diffusion.

Since the optically distinct core fragments are not necessarily in the center of the tourmaline grains (as in Fig. 3) zoning profiles may appear very different for grains even in the same sample. Consider the rim-to-rim compositional profiles across a pair of tourmaline grains that are cut perpendicular to the c-axis (Fig. 5). Grain 1, a type (2) tourmaline grain displaying continuous optical zoning, has a profile that is typical of continuously-zoned tourmalines. In contrast, grain 2, a type (3) tourmaline grain with a dark-brown core, displays a chemical zoning pattern that features a marked core-to-rim decrease in Fe, Ca, and Ti and an increase in Mg and Al. The most significant difference is that the Ca core-rim zoning pattern is in the opposite direction in the two grains. The core of grain 2 must have originated in a different environment (or provenance) than the core of grain 1. Despite the different zoning patterns in the interior of the crystals, the rim compositions of both grains are essentially the same. This suggests that the outermost portion of the tourmaline approached chemical equilibrium with the matrix minerals at the $P-T$ conditions of metamorphism.

Table 3. Representative microprobe analyses of tourmaline from NW Maine

	a9-66			b30-66		c16-66			1711/4	
	rim	core[*]	core[**]	rim	core[**]	rim	core[**]	core[*]	rim	core[**]
B_2O_3	10.65[***]	10.72	10.50	10.40	10.26	10.60	10.40	10.54	10.54	10.29
SiO_2	35.96	36.59	36.12	35.53	36.08	36.35	35.47	36.50	35.52	35.76
Al_2O_3	33.81	33.18	30.29	32.30	28.74	33.00	29.89	31.67	33.16	30.45
TiO_2	0.67	0.75	1.59	0.82	0.44	0.79	1.02	1.00	0.79	0.27
FeO	6.05	7.06	8.52	7.48	9.45	4.95	10.05	7.08	6.36	14.94
MnO	0.00	0.03	0.02	0.04	0.08	0.05	0.16	0.06	0.00	0.02
MgO	6.62	6.47	6.57	5.67	6.72	7.13	6.28	6.58	6.71	2.85
CaO	0.41	0.44	0.66	0.51	0.29	0.38	1.56	0.21	0.44	0.21
Na_2O	2.08	2.09	2.24	1.95	2.69	2.04	1.67	2.12	2.01	2.23
K_2O	0.05	0.05	0.06	0.02	0.03	0.02	0.08	0.03	0.04	0.07
Total	96.30	97.38	96.57	94.72	94.78	95.31	96.58	95.79	95.57	97.09

Structural formula on the basis of 29 oxygens

B	3.000	3.000	3.000	3.000	3.000	3.000	3.000	3.000	3.000	3.000
Si	5.868	5.933	5.977	5.938	6.114	5.959	5.929	6.018	5.855	6.044
Al_T	0.132	0.067	0.023	0.062	0.000	0.041	0.071	0.000	0.145	0.000
Al_Z	6.000	6.000	5.887	6.000	5.742	6.000	5.819	6.000	6.000	6.000
Al_Y	0.373	0.277	0.000	0.301	0.000	0.337	0.000	0.156	0.299	0.067
Ti	0.082	0.091	0.198	0.103	0.056	0.097	0.128	0.124	0.098	0.034
Fe	0.826	0.957	1.179	1.045	1.339	0.679	1.405	0.976	0.877	2.112
Mn	0.000	0.004	0.003	0.006	0.011	0.007	0.023	0.008	0.000	0.003
Mg	1.610	1.564	1.620	1.412	1.697	1.742	1.564	1.617	1.648	0.718
Y Total	2.891	2.893	3.000	2.862	3.104	2.862	3.120	2.882	2.922	2.934
Ca	0.072	0.076	0.117	0.091	0.053	0.067	0.279	0.037	0.078	0.038
Na	0.658	0.657	0.719	0.632	0.884	0.648	0.541	0.678	0.642	0.731
K	0.010	0.010	0.013	0.004	0.006	0.004	0.017	0.006	0.008	0.015
X Total	0.740	0.744	0.848	0.727	0.943	0.719	0.838	0.721	0.729	0.784

[*] Core composition in an area displaying continuous zoning.

[**] Core composition in an area displaying discontinuous zoning.

[***] The weight percent of B_2O_3 is calculated assuming 3 boron atoms in the structural formula.

Tourmaline rim relations. A more quantitative evaluation of the approach to equilibrium by the tourmaline rims can be made by considering the element partitioning between the tourmaline rims and the matrix minerals. Plots of the Mg/Fe ratios of the tourmaline rims versus the coexisting biotites (Fig. 6) and chlorites (Fig. 7) show that there is systematic element partitioning for these cations. Na–Ca partitioning between tourmaline rims and plagioclase is also regular (Fig. 8). These systematic relations suggest that the tourmaline rims have closely approached equilibrium with the matrix phases.

The partition coefficients for tourmaline rims and various matrix phases are given in Table 4. The high values of the partition coefficients demonstrate that the tourmaline rims have the highest Mg/Fe and Na/Ca ratios of any of the phases in the metapelites. Based on these observations, then, the Mg/Fe ratios in the minerals in the staurolite-grade pelitic schists proceed as follows: tourmaline rim > cordierite > chlorite > biotite > staurolite > garnet > ilmenite.

As demonstrated in Figures 6–8 tourmaline rim compositions show a significant range in the Mg/Fe and Na/Ca
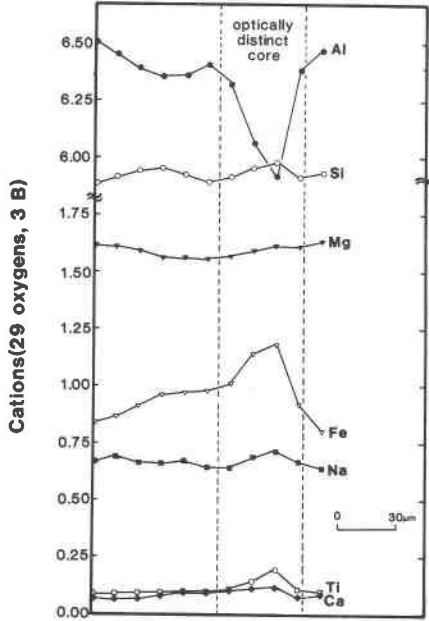
Fig. 4. Quantitative microprobe traverse across an optically discontinuously zoned tourmaline (section A–A′ in Fig. 3). The cations are calculated on the basis of 29 oxygen and 3 boron atoms in the structural formula. Based on replicate analyses, analytical uncertainties are typically less than 0.01 cation units.
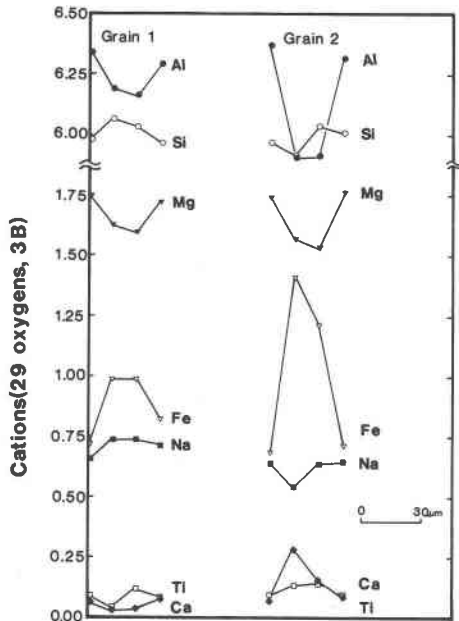

Fig. 5. Microprobe traverses across two tourmaline grains found within 1 mm of one another. The grains show different styles of zoning. Despite the differences in the internal zoning the compositions at the rims are essentially the same.
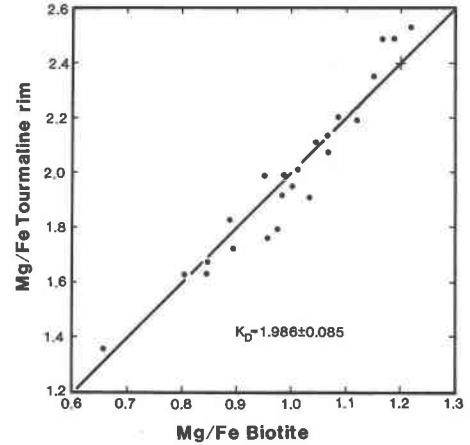
Fig. 6. Mg–Fe partitioning between biotite and coexisting tourmaline rims. The uncertainties due to analytical precision are shown by the horizontal and vertical bars.

ratios. However, a survey of the rim compositions indicates that the amounts of Si, Al, and Ti are relatively constant (Table 5). If the compositions of the tourmaline rims are plotted on an Al–Fe(tot)–Mg diagram (Fig. 9) the data cluster on a line of nearly constant Al. These data fall well within the field which has been defined for metapelites with a coexisting Al-saturating phase. This observation supports the contention that the saturating Al-, Si-, and Ti-phases maintain these cations at constant levels in the tourmaline rims at the constant P–T conditions of these rocks. A similar trend is found if the tourmaline rim compositions are plotted on a Ca–Fe(tot)–Mg diagram (Fig. 10). The slightly varying Ca values reflect the restricted plagioclase composition.

A general indication of the amount of dehydroxylation in the tourmaline rims can be gained by considering the average rim compositions. If the average tourmaline rim
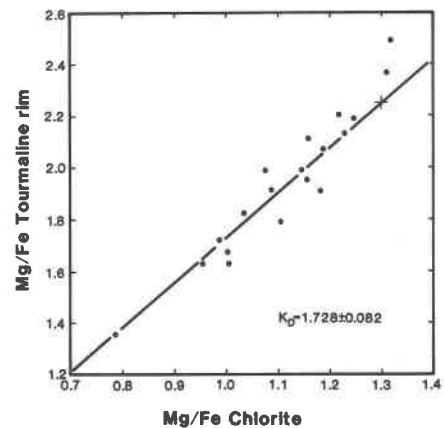

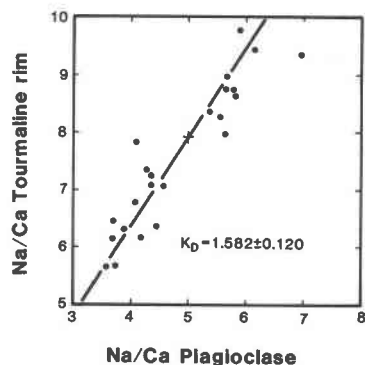Fig. 7. Mg–Fe partitioning between chlorite and coexisting tourmaline rims.

Fig. 8. Na–Ca partitioning between plagioclase and coexisting tourmaline rims.

Table 5. Variation in tourmaline rim compositions

	Range	Mean
Mg/Fe	1.359-2.533	2.001(0.299)[*]
Na/Ca	5.691-9.726	7.757(1.190)
Si	5.869-5.990	5.929(0.035)
Al_T	0.131-0.010	0.071(0.035)
Al_Z	6.000	6.000
Al_Y	0.245-0.370	0.312(0.035)
Ti	0.077-0.100	0.090(0.005)
F	0.062-0.155	0.093(0.028)
ΣY	2.802-2.906	2.861(0.021)[**]
ΣX	0.703-0.758	0.724(0.014)

[*]The estimated standard deviation is given in parentheses.

[**]Average tourmaline rim formula (on the basis of 29 oxygen and 3 boron atoms):

$$(Na_w Ca_x \square_{0.276})(Mg_y Fe_z Ti_{0.090} Al_{0.312} \square_{0.139})Al_{6.0}$$
$$(Si_{5.929} Al_{0.071})(BO_3)_3 O_{18}(OH_{3.907} F_{0.093})$$

$w=0.616-0.657$ $x=0.108-0.067$
$y=1.417-1.763$ $z=1.042-0.696$

Average tourmaline rim formula (on the basis of 3 boron atoms and a full occupancy of 3 cations in the Y site):

$$(Na_{w'} Ca_{x'} \square_{0.269})(Mg_{y'} Fe_{z'} Ti_{0.091} Al_{0.427})Al_{6.0}$$
$$(Si_{5.984} Al_{0.016})(BO_3)_3 O_{18}(O_{0.458} OH_{3.449} F_{0.093})$$

$w'=0.622-0.663$ $x'=0.109-0.068$
$y'=1.430-1.779$ $z'=1.052-0.703$

formula is calculated on the basis of 29 oxygen and 3 boron atoms the total number of cations in the Y site is 2.861 (±0.021); implying vacancies in the Y site. Nonetheless structural determinations of tourmalines have not indicated that there are any Y site vacancies in tourmalines of the schorl-dravite series (Donnay and Barton, 1972; Foit and Rosenberg, 1977; Rosenberg and Foit, 1979). If, however, it is assumed that there is full Y site occupancy (i.e., no Y site vacancies) and charge balance is maintained by loss of a proton from the hydroxyl site, an average tourmaline rim composition can be recalculated (Table 5). This calculation shows that 11.5% of the hydroxyl in the hydroxyl site would be replaced by oxygen. This value represents the minimum amount of dehydroxylation since there will be additional proton loss if any of the Y site iron is trivalent or if Mg substitutes for Na in the X site. The significant amount of dehydroxylation which is implied by this calculation is consistent with the probable involvement of an aluminobuergerite substitution in the tourmaline rims. In addition, there are also vacancies in the X site reflecting a significant amount of alkali defect substitution.

Table 4. Partition coefficients for tourmaline rims and coexisting matrix phases

Element pair	Mineral pair	K_D[*]
Mg-Fe	tourmaline-biotite	1.986(0.085)[**]
Mg-Fe	tourmaline-chlorite	1.728(0.082)
Mg-Fe	tourmaline-garnet	13.94(0.72)
Mg-Fe	tourmaline-cordierite	1.236(0.068)
Mg-Fe	tourmaline-staurolite	10.29(1.25)
Na-Ca	tourmaline-plagioclase	1.582(0.120)

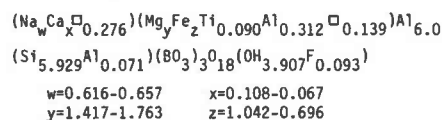[*] $K_D=(Mg/Fe)_{tour}/(Mg/Fe)_{pair}$ or $(Na/Ca)_{tour}/(Na/Ca)_{plag}$.

[**]The estimated standard deviations are given in parentheses.

Tourmaline core relations. The range, mean, and standard deviation of compositions of the continuously- and discontinuously-zoned cores are given in Table 6. As evidenced by the large range and standard deviations, both types of cores show considerably more compositional variation than the corresponding rim compositions.

Despite the increased compositional variability the continuously-zoned (type (2)) cores have several distinct compositional trends relative to the rims: (1) the Mg/Fe ratios are lower and the Na/Ca ratios are higher in these cores, (2) Si approaches the full six cations of the tetrahedral site and, conversely, tetrahedral Al approaches zero, (3) total Al decreases slightly. (4) Ti usually decreases. These relationships are illustrated qualitatively by the positions of the continuously-zoned cores relative to the field of the rims in the Al–Fe(tot)–Mg diagram (Fig. 9) and Ca–Fe(tot)–Mg diagram (Fig. 10). These data suggest that from the core to the rim there is a continuous increase in the $MgFe_{-1}$, $Al_2Mg_{-1}Si_{-1}$, $CaMgNa_{-1}Si_{-2}$, and $TiAl_2Mg_{-1}Si_{-2}$ components. These components probably increased during prograde growth of the tourmaline in the pelitic schists. These changes are analogous to the compositional changes observed in
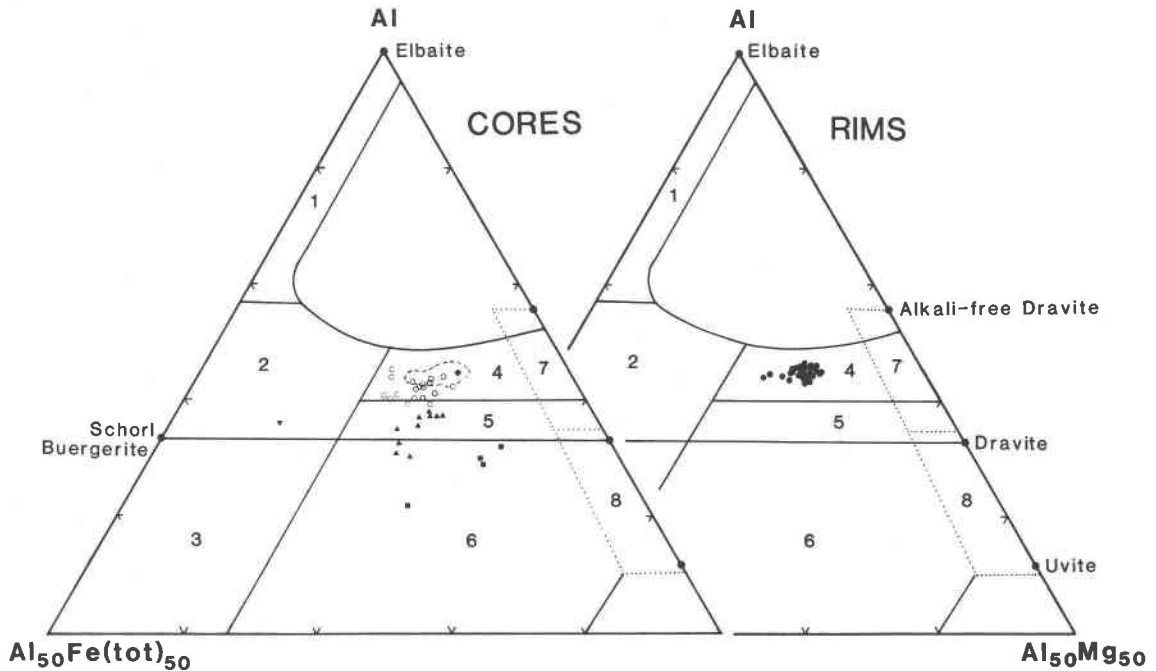
Fig. 9. Al–Fe(tot)–Mg diagram for tourmaline core and rim compositions from NW Maine. Most of the data cluster along a line of nearly constant Al content. The compositions of the tourmaline cores are divided into the continuously-zoned cores (O) and the four varieties of discontinuously-zoned cores as described in the text: variety 1 (▲); variety 2 (■); variety 3 (▼); and variety 4 (◆). The dashed line represents the field encompassed by the tourmaline rim compositions. The numbers in the fields corresponding to potential source rock types are defined in Fig. 1.

biotite, muscovite, and plagioclase from pelitic schists which increase in grade from garnet to staurolite grade (Guidotti and Sassi, 1976; Guidotti et al., 1977; Guidotti, 1978).

Core compositions from discontinuously-zoned (type (3)) tourmalines are extremely variable and show no relation between the Mg/Fe and Na/Ca ratios and the compositions of the coexisting matrix minerals. This type of core can be grouped into four broad compositional categories. Variety 1 has relatively high Fe contents usually with an excess of cations in the Y site and deficiency in the Z site. This implies that there is probably a significant amount of ferric iron substituting for Al. In addition, there is an increase in Ti but a decrease in X site vacancies relative to their rims. Variety 2, a less abundant type, is characterized by high Ca and Ti contents and typically high Mg/Fe ratios. It also has an Al deficiency in the Z site which is most likely due to a substantial uvite substitution. Variety 3, observed in a single grain, has a very low Mg/Fe ratio but relatively high Al levels. Variety 4, observed in a single grain, is very aluminous with lower Ca and Ti contents and higher Mg/Fe ratios relative to its rim.

If it is assumed that the discontinuous cores are detrital in origin, the chemistry of these discontinuously-zoned cores allows some constraints to be placed on the possi-

ble source rocks. In Figures 9 and 10, the variety 1 cores fall in the fields that suggest the tourmaline core formed in relatively Fe^{3+}-rich metapelites or metapsammites (probably with no graphite present) not containing an Al-saturating phase. The higher Ti contents imply that they formed at a different P,T condition and/or with a different Ti-saturating phase (such as rutile). The calcic and magnesian variety 2 cores fall in fields that suggest an environment which may be found in carbonate-bearing metapelites and metapsammites. The variety 3 core has a composition which falls well within the Li-poor granitoid field suggesting it was detritus from a granitoid pluton. Finally, the aluminous variety 4 core was probably derived from a pelitic schist which coexisted with relatively magnesian phases as well as an Al-saturating phase.

The sedimentary source region for the metapelites in the Rangeley quadrangle is presumed to be the Cambro-Ordivician strata of the Somerset Geanticline (Cady, 1968, 1969; Moench, 1973) which contains relatively oxidized horizons of metapelites, metaquartzites, and metacarbonates as well as a few granitic plutons. These rock types are good candidates for source rocks of the detrital tourmaline fragments. Krynine (1946) has noted that since tourmaline is extremely resistant to abrasion, it is common to find that even in a single sedimentary basin, due to mixing from several source areas, there may be a
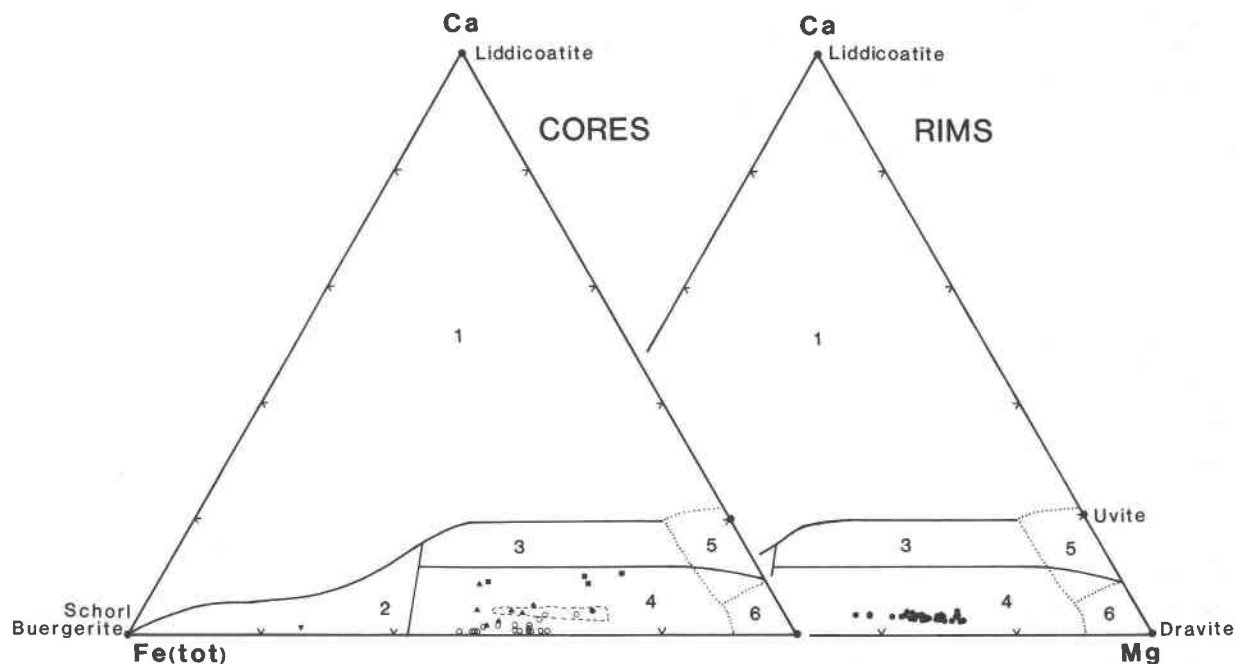
Fig. 10. Ca–Fe(tot)–Mg diagram for tourmaline core and rim compositions from NW Maine. The rim compositions plot in a narrow band at nearly constant Ca content. The symbols for the core data are given in Fig. 9. The dashed line represents the outline of the field encompassed by the tourmaline rim compositions. The numbers in the fields corresponding to potential source rock types are defined in Fig. 2.

collection of tourmaline grains of various types. Thus even in a small area tourmaline detritus from several source regions may be expected. These data suggest that detrital cores from tourmaline may provide information on the provenance of the sediments which predate metamorphism.

Development of tourmaline during metamorphism

In the staurolite-grade pelitic schists of NW Maine, tourmaline is dispersed throughout the rocks and there is no evidence that its development is due to externally-derived, B-rich fluids. The tourmaline must have been part of the original pelitic sediment and/or must have progressively developed during metamorphism of the pelites.

In most common metasediments the bulk of the boron is carried in the tourmaline contained in the rocks (Ethier and Campbell, 1977). However, the source of the boron in many sediments is somewhat problematic. In coarse clastic, sedimentary rocks tourmaline has often been observed as a mechanically-resistant detrital mineral (Pettijohn et al., 1973). In contrast, in fine-grained, argillaceous sedimentary rocks that are often relatively rich in boron (Ethier and Campbell, 1977), the bulk of the boron cannot be contained exclusively in the detrital tourmaline

grains. Instead, boron apparently (1) was in solution in sea water and held by adsorption onto the surface of clay minerals (especially illite), (2) substituted for silicon in the tetrahedral sites of the clay minerals or for carbon in

Table 6. Variation in tourmaline core compositions

	Continuously-zoned cores		Discontinuously-zoned cores	
	Range	Mean	Range	Mean
Mg/Fe	0.982–1.696	1.366(0.219)*	0.340–3.208	1.595(0.681)
Na/Ca	6.527–116.8	42.73(28.75)	0.956–19.216	8.384(6.911)
Si**	5.884–6.084	6.013(0.050)	5.874–6.114	5.981(0.069)
Al_T	0.000–0.116		0.000–0.126	
Al_Z	6.000	6.255(0.096)	5.354–6.000	5.934(0.267)
Al_Y	0.137–0.423		0.000–0.408	
Ti	0.025–0.100	0.065(0.021)	0.033–0.230	0.115(0.057)
F	0.057–0.149	0.095(0.038)	0.069–0.198	0.119(0.051)
ΣY	2.818–2.942	2.879(0.042)	2.808–3.594	3.041(0.208)
ΣZ	0.589–0.800	0.707(0.048)	0.707–0.943	0.831(0.067)

*The estimated standard deviations are given in parentheses.

**The structural formula is calculated on the basis of 29 oxygen and 3 boron atoms

dolomite, or (3) was redistributed as a result of post-depositional movement of a boron-rich fluid (Stubican and Roy, 1962; Eager and Spears, 1966; Lerman, 1966; Cody, 1971; Abraham et al., 1972; Wadhawan and Roonwal, 1977; Ricketts, 1978; Slack, 1982). Consequently boron can be concentrated in sediments by several mechanisms.

The following scenario is proposed for the development of tourmaline during metamorphism of the pelitic sediments of NW Maine. With an increase in temperature the boron is released from the clays and made available to interstitial fluids to react with the coexisting aluminosilicate minerals in the sediment to form tourmaline. This is initially reflected in the development of authigenic tourmaline during the late stages of diagenesis forming as overgrowths on detrital tourmaline grains and/or as newly-developed tourmaline crystals. With a further increase in temperature, more of the boron released forms additional tourmaline that armors the preexisting cores. Thus, any detrital core tends to be preserved by the tourmaline overgrowths. At high grades of metamorphism, the tourmaline grains tend to become more chemically homogeneous. For instance, Frey (1969) noted that with increase in grade from greenschist to amphibolite facies tourmaline in metapelites has an increasingly greater proportion of metamorphic overgrowth to detrital core. The development of metamorphic overgrowths gives a mechanism that can produce the type (3) zoning patterns. Since the chemical zoning mimics the compositional evolutions of the matrix minerals, the continuously-zoned tourmaline (type (2)) probably developed during progressive metamorphism whereas the unzoned type (1) tourmaline core probably developed at nearly constant P,T conditions.

Conclusions

The investigation of the chemical characteristics of accessory tourmaline in staurolite grade metapelitic schists from NW Maine demonstrates that tourmaline can be a useful petrogenetic indicator mineral. The rims of the tourmaline grains appear to be in chemical equilibrium with the matrix minerals and have high regular partition coefficients between tourmaline rims and matrix minerals. However, care must be exercised in comparing partition coefficients in rocks from different regions to those of this study. It must be certain that the rim of the tourmaline is used for element partitioning and that compositional complexities in tourmaline are minimized by considering tourmalines coexisting with the appropriate saturating phases.

The refractory nature of the tourmaline is reflected in the strong zoning patterns and detrital cores that apparently have not undergone substantial chemical changes despite being subjected to staurolite-grade metamorphism. Consequently, by considering the nature of the chemical zoning, tourmalines can be extremely useful probes into the history of the rocks in which they are found.

Finally, it is urged that tourmaline become a mineral that is routinely considered and carefully analyzed during any petrologic study. As more information becomes available, its utility and limitations to petrogenesis will become more apparent.

References

Abraham, K., Mielke, H., and Povondra, P. (1972) On the enrichment of tourmaline in metamorphic sediments of the Arzberg Series, W. Germany (NE Bavaria). Neues Jahrbuch für Mineralogie, Monatshefte, 209–219.

Abraham, K. and Schreyer, W. (1973) Petrology of a ferruginous hornfels from Riekensgluck, Harz Mountains, Germany. Contributions to Mineralogy and Petrology, 40, 275–292.

Ackermand, D. and Morteani, G. (1977) The chemistry of the garnets, chlorite, biotite, and tourmaline in the Steinkogel Schist (Salzburg, Austria): the geological history of the central Eastern Alps. Neues Jahrbuch Geologische und Paleontologie, Abhandlungen, 154, 367–385.

Albee, A. L. and Ray, L. (1970) Correction factors for electron probe microanalysis of silicates, oxides, carbonates, phosphates, and sulfates. Analytical Chemistry, 42, 1408–1414.

Awasthi, N. (1961) Authigenic tourmaline and zircon in the Vindhyan formations of Sone Valley, Mizapur District, Uttar Pradesh, India. Journal of Sedimentary Petrology, 31, 482–484.

Babu, S. K. (1970) Mineralogy of achroite (colourless tourmaline), from a pegmatite near Ajmer. Current Science, 39, 154–156.

Baker, J. H. and de Groot(1983) Proterozoic seawater–felsic volcanics interaction W. Bergslagen, Sweden: Evidence for high REE mobility and its implications. Contributions to Mineralogy and Petrology, 82, 119–130.

Barton, R., Jr. (1969) Refinement of the crystal structure of buergerite and absolute orientation of tourmalines. Acta Crystallographica, B25, 1524–1532.

Bence, A. E. and Albee, A. L. (1968) Empirical correction factors for the electron microanalysis of silicates and oxides. Journal of Geology, 76, 382–403.

Benjamin, R. E. K. (1969) An axinite-epidote-tourmaline vein cutting amphibolite, western Connemara, Eire. Mineralogical Magazine, 36, 747–750.

Black, P. M. (1971) Tourmalines from Cuvier Island, New Zealand. Mineralogical Magazine, 38, 374–376.

Bouska, V., Povondra, P., and Lisy, E. (1973) Uvite from Hnusta, Czechoslavakia. Acta Universitatis Carolinae-Geologica, 3, 163–170.

Bowman, H. L. (1902) Occurrence of minerals at Haddam Neck, Connecticutt, USA. Mineralogical Magazine, 13, 108–111.

Bradley, J. E. S. and Bradley, O. (1953) Observations on the colouring of pink and green zoned tourmaline. Mineralogical Magazine, 30, 26–38.

Bridge, P. J., Daniels, J. L. and Pryce, M. W. (1977) The dravite crystal bonanza of Yinnietharra, Western Australia. Mineral Record, 8, 109–110.

Bruce, E. L. (1917) Magnesian tourmaline from Renfrew, Ontario. Mineralogical Magazine, 18, 133–135.

Burns, R. G. (1982) The blackness of schorl: Fe^{2+}–Fe^{3+} electron delocalization in tourmalines. Transactions of the American Geophysical Union, 63, 1142.

Cady, W. H. (1968) Tectonic setting and mechanism of the Taconic slide. American Journal of Science, 266, 563–578.

Cady, W. H. (1969) Regional tectonic synthesis of northwestern New England and adjacent Quebec. Geological Society of America Memoir 120.

Chaudry, M. N. and Howie, R. A. (1976) Lithium tourmalines from the Meldon aplite, Devonshire, England. Mineralogical Magazine, 40, 747–751.

Cody, R. (1971) Adsorption and reliability of trace elements as environmental indicators for shales. Journal of Sedimentary Petrology, 41, 461–471.

Coelho, I. S. (1948) Turmalina fibrosa da "Mina do Cruzeiro" Santa Maria do Suassui, Minas Gerais. Mineracao e Metalurgia, Rio de Janeiro, 13, 49–53.

Deer, W. A., Howie, R. A., and Zussman, J. (1962) An Introduction to the Rock-forming Minerals. Longmans, Green and Co. Ltd., London.

Donnay, G. and Barton, R. Jr. (1972) Refinement of the crystal structure of elbaite and the mechanism of tourmaline solid solution. Tschermaks Mineralogische und Petrographische Mitteilungen, 18, 273–286.

du Rietz, T. (1935) Peridotites, serpentinites, and soapstones of northern Sweden, with special reference to some occurrences on northern Jamtland. Geologiska Foreningens i Stockholm Forhandlingar, 57, 133–260.

Dunn, P. J. (1977) Chromium in dravite. Mineralogical Magazine, 41, 408–410.

Dunn, P. J., Appleman, D. E., and Nelen, J. E. (1977a) Liddicoatite, a new calcium end-member of the tourmaline group. American Mineralogist, 62, 1121–1124.

Dunn, P. J., Appleman, D., Nelen, J. A., and Norberg, J., (1977b) Uvite, a new (old) common member of the tourmaline group and its implications to collectors. Mineral Record, 8, 100–108.

Eagar, R. M. C. and Spears, D. A. (1966) Boron content in relation to organic carbon and to paleosalinity in certain British Upper Carboniferous sediments. Nature, 209, 172–181.

El-Hinnawi, E. E. and Hofmann, R. (1966) Optical and chemical investigation of nine tourmalines (elbaite). Neues Jahrbuch für Mineralogie, Monatshefte, 80–88.

Ethier, V. G. and Campbell, F. A. (1977) Tourmaline concentrations in Proterozoic sediments of the southern Cordillera of Canada and their economic significance. Canadian Journal of Earth Sciences, 14, 2348–2363.

Fieremans, M. and Paepe, P. D. (1982) Genesis of tourmalinites from Belgium: petrographical and chemical evidence. Mineralogical Magazine, 46, 95–102.

Foit, F. F., Jr. and Rosenberg, P. E. (1977) Coupled substitutions in the tourmaline group. Contributions to Mineralogy and Petrology, 62, 109–127.

Foit, F. F., Jr. and Rosenberg, P. E. (1979) The structure of vanadium-bearing tourmaline and its implications regarding tourmaline solid solutions. American Mineralogist, 64, 788–798.

Foord, E. E. and Mills, B. A. (1978) Biaxiality in 'isometric' and 'dimetric' crystals. American Mineralogist, 63, 316–325.

Fortier, S. and Donnay, G. (1975) Schorl refinement showing composition dependence of the tourmaline structure. Canadian Mineralogist, 13, 173–177.

Frey, M. (1969) Die metamorphose des Keupers vom Tafeljura bis zum Lukmanier-Gebeit (Veranderungen tonig-mergeliger Geteine von Bereich der Diagenese bis zur staurolith-zone). Beitraege zur Geologischen Karte der Scheiz, 137, 1–160.

Frondel, C., Biedl, A., and Ito, J. (1966) New type of ferric iron tourmaline. American Mineralogist, 51, 1501–1505.

Gautier, D. L. (1979) Preliminary report of authigenic, euhedral tourmaline crystals in a productive gas reservoir of the Tiger Ridge Field, north-central Montana. Journal of Sedimentary Petrology, 49, 911–916.

Gorelikova, N. V., Perfil'yev, Yu. D., and Bubeshkin, A. M. (1978) Mössbauer data on distribution of Fe ions in tourmaline. International Geology Review, 20, 982–990.

Guidotti, C. V. (1970) Metamorphic petrology, mineralogy, and polymetamorphism in a portion of NW Maine. In G. M. Boone, Ed., The Rangeley Lakes-Dead River Basin Region, Western Maine, New England Intercollegiate Geological Conference Guidebook B-2, 1–29.

Guidotti, C. V. (1974) Transition from staurolite to sillimanite zone Rangeley quadrangle, Maine. Geological Society of America Bulletin, 85, 475–490.

Guidotti, C. V. (1978) Compositional variation of muscovite in medium- to high-grade metapelites of northwestern Maine. American Mineralogist, 63, 878–884.

Guidotti, C. V., Cheney, J. T., and Guggenheim, S. (1977) Distribution of titanium between coexisting muscovite and biotite in pelitic schists from northwestern Maine. American Mineralogist, 62, 438–448.

Guidotti, C. V. and Sassi, F. P. (1976) Muscovite as a petrogenetic indicator mineral in pelitic schists. Neues Jahrbuch für Mineralogie, Abhandlungen, 127, 97–142.

Henry, D. J. (1981) Sulfide-silicate relations of the staurolite grade pelitic schists, Rangeley Quadrangle, Maine. Ph.D. dissertation, University of Wisconsin-Madison.

Henry, D. J. and Guidotti, C. V. (1981) Implications of the sulfide-silicate interactions in staurolite grade metapelites in NW Maine. Transactions of the American Geophysical Union, 62, 435.

Henry, D. J. and Guidotti, C. V. (1982) Sulfide–silicate–fluid interactions in metapelitic rocks: internal vs. external control. Geological Association of Canada and Mineralogical Association of Canada Program with Abstracts, 7, 55.

Hermon, E., Simkin, D. J., Donnay, G., and Muir, W. B. (1973) The distribution of Fe^{2+} and Fe^{3+} in iron-bearing tourmalines: a Mössbauer study. Tschermaks Mineralogische und Petrographische Mitteilungen, 19, 124–132.

Holdaway, M. J., Guidotti, C. V., Novak, J. M., and Henry, W. E. (1982) Polymetamorphism in medium- to high-grade pelitic metamorphic rocks west-central Maine. Bulletin of the Geological Society of America, 93, 572–584.

Holgate, N. (1977) Tourmaline from amphibolized gabbro at

Hanter Hill, Radnorshire. Mineralogical Magazine, 41, 124–127.

Hutcheon, I., Gunter, A. E., and Lecheminant, A. N. (1977) Serendibite from Penrhyn Group marble, Melville Peninsula, District of Franklin. Canadian Mineralogist, 15, 108–112.

Jan, M. Q., Kempe, D. R. C., and Symes, R. F. (1972) A chromian tourmaline from Swat, West Pakistan. Mineralogical Magazine, 38, 756–759.

Jedwab, J. (1962) Tourmaline zinifere dan une pegmatite de Muike (Congo). Bulletin de la Societe Belge de Geologie, 71, 132–135.

Jones, B. G., Carr, P. F., and Condliffe, E. (1981) Ferrian tourmaline from Bungonia, New South Wales. Journal of the Geological Society of Australia, 28, 13–17.

Kitahara, J. (1966) On dravite (Mg-tourmaline) from the Hirose mine, Tottori Prefecture. Journal of the Japanese Association of Mineralogists Petrologists, and Economic Geologists, 56, 228–233.

Korovushkin, V. V., Kuzmin, V. L., and Belov, V. F. (1979) Mössbauer studies of structural features in tourmaline of various geneses. Physics and Chemistry of Minerals, 4, 209–220.

Kramer, H. and Allen, R. D. (1954) Analyses and indices of refraction of tourmaline from fault gouge near Barstow, San Bernadino County, California. American Mineralogist, 39, 1020–1022.

Krynine, P. D. (1946) The tourmaline group in sediments. Journal of Geology, 54, 65–87.

Leckebusch, R. (1978) Chemical composition and colour of tourmalines from Darre Pech (Nuristan, Afganistan). Neues Jahrbuch für Mineralogie, Abhandlungen, 133, 53–70.

Lerman, A. (1966) Boron in clays and estimation of paleosalinities. Sedimentology, 6, 267–286.

MacRae, N. D. and Kullerud, G. (1972) Preliminary investigation of almandine–sulfur–water at 700°C and 1 kb. Canadian Mineralogist, 11, 563–566.

Mader, D. (1980) Tourmaline authigenesis in carbonate-rock breccias from the upper Bunter of the northern Triev Bay; western Eifel, Aufschluss, 31, 249–256.

Manning, D. A. C. (1982) Chemical and morphological variation in tourmalines from the Hub Kapong batholith of peninsular Thailand. Mineralogical Magazine, 45, 139–147.

Moench, R. H. (1973) Down-basin fault-fold tectonics in western Maine with comparison to the Taconic Klippe. In K. A. DeJong and R. Scholten, Eds., Gravity and Tectonics. p. 327–342. Interscience, New York.

Moench, R. H. and Zartman, R. E. (1976) Chronology and styles of multiple deformation, plutonism, and polymetamorphism in the Merrimack Synclinorium of western Maine. In P. C. Lyons and A. H. Brownlow, Eds., Studies in New England Geology, Geological Society of America Memoir 146, 203–238.

Mukherjee, S. (1969) The chrome-tourmaline from Nausahi, Keonjhar District, Orissa. Quarterly Journal of the Geological Mining and Metallurgical Society of India, 40, 119–121.

Neiva, A. M. R. (1974) Geochemistry of tourmaline (schorlite) from granites, aplites and pegmatites from northern Portugal. Geochimica et Cosmochimica Acta, 38, 1307–1317.

Nemec, D. (1968) Fluorine in tourmalines. Contributions to Mineralogy and Petrology, 20, 235–243.

Novak, F. and Zak, L. (1970) Dravite asbestos from Chlavetice. Acta Universitatis Carolinae-Geologica, 1, 27–44.

Nuber, B. and Schmetzer, K. (1979) The lattice position of Cr^{3+} in tourmaline; structural refinement of a chromium-rich Mg–Al–tourmaline. Neues Jahrbuch für Mineralogie, Abhandlungen, 137,184–197.

Ontoev, D. O. (1956) On the composition of certain ore-forming tourmalines. Transactions of the Institute for the Geology of Ore-deposits, Petrography, Mineralogy, and Geochemistry, 3, 340–346.

Osberg, P. H. (1978) Synthesis of the geology of the northeastern Appalachians, USA. Geological Survey of Canada, Paper 78-13, 137–147.

Otroshchenko, V. D., Dusmatov, V. D., Khorvat, V. A., Akramov, M. B., Morozov, S. A., Otroshchenko, L. A., Khalilov, M. Kh., Kholopov, N. P., Vinogradov, O. A., Kudryavtsev, A. S., Kabanova, L. K., and Sushchinskiy, L. S. (1972) Tourmalines in Tien Shan and the Pamirs, Soviet Central Asia. International Geology Review, 14, 1173–1181.

Pagliani, G. (1949) La turmalina di Beura. Atti della Societa Italiana di Scienze Naturali e del Museo Civico di Storia Naturale di Milano, 88, 191–198.

Peltola, E., Vourelainen, Y., and Hakli, T. A. (1968) A chromian tourmaline from Outokumpu, Finland. Bulletin of the Geological Society of Finland, 40, 35–38.

Pettijohn, F. J., Potter, P. E. and Siever, R. (1973) Sand and Sandstones. Springer-Verlag, New York.

Povondra, P. (1981) The crystal chemistry of tourmalines of the schorl-dravite series. 1981 Acta Universitatis Carolinae-Geologica, 223–264.

Power, G. M. (1968) Chemical variation in tourmalines from South-West England. Mineralogical Magazine, 36, 1078–1089.

Raheim, A. (1977) Petrology of the Strathgordon area, western Tasmania: Si^{4+}-content of phengite mica as a monitor of metamorphic grade. Journal of the Geological Society of Australia, 24, 329–338.

Rath, R. and Puchelt, H. (1957) Indigolith von Usakos. Neues Jahrbuch für Mineralogie, Monatshefte, 206–209.

Rath, R. and Puchelt, H. (1959) Dravit von Gouverneur. Neues Jahrbuch für Mineralogie, Monatshefte, 22–24.

Ricketts, B. D. (1978) Authigenic tourmaline from the Middle Precambrian Belcheger group, Northwest Territories, Canada. Bulletin of Canadian Petroleum Geology, 26, 543–550.

Rosenberg, P. E. and Foit, F. F. Jr. (1979) Synthesis and characterization of alkali-free tourmaline. American Mineralogist, 64, 180–186.

Sahama, Th. G., von Knorring, O., and Tornoos, R. (1979) On tourmaline. Lithos, 12, 109–114.

Sandrea, A. (1949) Sur une variety de tourmaline sodo-manganesifere dans des filons de pegmatite des environ des Roscoff. Comptes Rendus Hebdomodaires des Seances de l'Academie des Sciences, Paris, 228, 1142–1143.

Schmetzer, K., Nuber, B., and Abraham, K. (1979) Crystal chemistry of magnesium-rich tourmalines. Neues Jahrbuch für Mineralogie, Abhandlungen, 136, 93–112.

Schreyer, W., Abraham, K., and Kulke, H. (1980) Natural sodium phlogopite with potassium phlogopite and sodian aluminian talc in a metamorphic evaporite sequence from Derrag, Tell Atlas, Algeria. Contributions to Mineralogy and Petrology, 74, 223–233.

Schreyer, W., Werding, G. and Abraham, K. (1981) Corundum-fuchsite rocks in greenstone belts of southern Africa: petrology, geochemistry, and possible origin. Journal of Petrology, 22, 191–231.

Serdyuchenko, D. P. (1976) Archean tourmaline-bearing and

other metasedimentary gneisses of the Azov region, as related to their paleogeographic environment of formation. Doklady, Academy of Sciences of the USSR, Earth Sciences Sections, 227, 90–93.

Slack, J. F. (1982) Tourmaline in Appalachian-Caledonian massive sulphide deposits and its exploration significance. Transactions/section B of the Institution of Mining and Metallurgy, 91, B81–B87.

Slivko, M. N. (1959) Manganese tourmalines. Mineralogichesky sbornik, Lvovskogo geologocheskogo obshchestva, 13, 139–148.

Snetsinger, K. G. (1966) Barium-vanadium muscovite and vanadium tourmaline from Mariposa County, California. American Mineralogist, 51, 1623–1639.

Staatz, M. H., Murata, K. J., and Glass, J. J. (1955) Variation of composition and physical properties of tourmaline with its position in the pegmatite. American Mineralogist, 40, 789–804.

Stubican, V. and Roy, R. (1962) Boron substitution in synthetic micas and clays. American Mineralogist, 47, 1166–1173.

Thompson, A. B., Lyttle, P. T., and Thompson, J. B. (1977) Mineral reactions and A–Na–K and A–F–M facies types in the Gassetts schist, Vermont. American Journal of Science, 277, 1124–1151.

Thompson, J. B., Jr. (1972) Oxides and sulfides in regional metamorphism of pelitic schists. Proceedings of the 24th International Geological Congress, Montreal, Section 10, 27–35.

Thompson, J. B., Jr. (1982) Composition space: an algebraic and geometric approach. In J. M. Ferry, Ed., Characterization of Metamorphism through Mineral Equilibria. Reviews in Mineralogy, 10, 1–31.

Thompson, J. B., Jr., Laird, J., and Thompson, A. B. (1982) Reactions in amphibolite, greenschist and blueschist. Journal of Petrology, 23, 1–27.

Tsang, T. and Ghose, S. (1973) Nuclear magnetic resonance of ^1H, ^7Li, ^{11}B, ^{23}Na and ^{27}Al in tourmaline (elbaite). American Mineralogist, 58, 224–229.

Tsang, T., Thorpe, A. N., and Donnay, G. (1971) Magnetic susceptibility and triangular exchange coupling in the tourmaline mineral group. Journal of the Physics and Chemistry of Solids, 32, 1441–1448.

von Knorring, O. (1970) Mineralogical and geochemical aspects of pegmatites from orogenic belts of equatorial and southern Africa. In Clifford, T. N. and Gass, I. G., Eds., African Magmatism and Tectonics, p. 157–184. Oliver and Boyd, Edinburgh.

Vrana, S. (1979) A polymetamorphic assemblage of grandidierite, kornerupine, Ti-rich dumortierite, tourmaline, sillimanite, and garnet. Neues Jahrbuch für Mineralogie, Monatshefte, 22–33.

Wadhawan, S. K. and Roonwal, G. S. (1977) Genetic significance of tourmaline associated with sulphide mineralization at Zawar area, Udaipur, Rajasthan, India. Neues Jahrbuch für Mineralogie, Monatshefte, 233–237.

Walenta, K. and Dunn, P. J. (1977) Ferridravite, a new mineral of the tourmaline group from Bolivia. American Mineralogist, 64, 945–948.

Wang, S. and Xue-yen, H. (1966) A new variety of dravite and its significance in mineralogy. Kexue Tongbao, 17, 91–96.

Williams, G. A. (1891) Minerals from Maryland. Mineralogical Magazine, 9, 247.

Wilson, G. C. and Long, J. V. P. (1983) The distribution of lithium in some Cornish minerals: ion microprobe measurements. Mineralogical Magazine, 47, 191–199.

Zen, E. (1981) Metamorphic mineral assemblages of slightly calcic pelitic rocks in and around the Taconic Allochthon, southwestern Massachusetts and adjacent Connecticut and New York. United States Geological Survey Professional Paper, 1113, 1–128.

Appendix 1

Source papers for tourmaline analyses

Tourmaline compositional data used to define the fields in the Al–Fe(tot)–Mg and Ca–Fe(tot)–Mg diagrams were taken from: Williams, 1891; Bowman, 1902; Bruce, 1917; du Rietz, 1935; Coelho, 1948; Pagliani, 1949; Sandrea, 1949; Bradley and Bradley, 1952; Kramer and Allen, 1954; Staatz et al., 1955; Ontoev, 1956; Rath and Puchelt, 1957, 1959; Slivko, 1959; Deer et al., 1962; Jedwab, 1962; El-Hinnawi and Hofmann, 1966; Frondel et al., 1966; Kitahara, 1966; Snetsinger, 1966; Wang and Xue-yen, 1966; Peltola et al., 1968; Power, 1968; Mukherjee, 1969; Babu, 1970; Novak and Zak, 1970; von Knorring, 1970; Otroschenko et al., 1971; Tsang et al., 1971; Abraham et al., 1972; Donnay and Barton, 1972; Jan et al., 1972; MacRae and Kullerud, 1972; Abraham and Schreyer, 1973; Bouska et al., 1973; Neiva, 1974; Fortier and Donnay, 1975; Chaudry and Howie, 1976; Serdyuchenko, 1976; Ackermand and Morteani, 1977; Bridge et al., 1977; Dunn, 1977; Dunn et al. 1977a, 1977b; Ethier and Campbell, 1977; Holgate, 1977; Hutcheon et al., 1977; Raheim, 1977; Foord and Mills, 1978; Gorelikova et al., 1978; Leckebusch, 1978; Foit and Rosenberg, 1979; Sahama et al., 1979; Schmetzer et al., 1979; Vrana, 1979; Walenta and Dunn, 1979; Schreyer et al., 1980, 1981; Povondra, 1981; Jones et al., 1982; Manning, 1982; Baker and de Groot, 1983; Wilson and Long, 1983; Henry (unpublished data).